Screw behavior in large diameter slewing bearing assemblies: Numerical and experimental analyses

Article *in* International Journal on Interactive Design and Manufacturing (IJIDeM) · April 2007

DOI: 10.1007/s12008-007-0003-7

CITATIONS
23

READS
907

3 authors:

Zouhair Chaib
Technical Centre for Mechanical Industry
6 PUBLICATIONS **160** CITATIONS
SEE PROFILE

Alain Daidié
Institut National des Sciences Appliquées de Toulouse
71 PUBLICATIONS **638** CITATIONS
SEE PROFILE

Dimitri Leray
Institut National des Sciences Appliquées de Toulouse
18 PUBLICATIONS **135** CITATIONS
SEE PROFILE

Int J Interact Des Manuf (2007) 1:21–31
DOI 10.1007/s12008-007-0003-7

ORIGINAL PAPER

Screw behavior in large diameter slewing bearing assemblies: numerical and experimental analyses

Zouhair Chaib · Alain Daidié · Dimitri Leray

Received: 1 October 2005 / Revised: 20 December 2005 / Accepted: 12 September 2006 / Published online: 15 March 2007

Abstract This paper investigates the behavior of large diameter bearing bolted joint in order to evaluate fatigue resistance of the screws. Based on experimental results, a sector of a slewing bearing is modeled using 3D finite elements. The model is built via hypothesis of sine-distributed efforts on the roller tracks. The simulations are carried out for the most loaded screw, which is located in the symmetry plane. Experimental measures on equipped screws are checked against numerical 3D simulations. This validates the numerical modeling method. Then the numerical model is used to evaluate the influence of several geometrical and physical parameters. The preload intensity reveals to be the major parameter. The bushes' height affects load filtering and improves fatigue strength of the screws. The height of the mounting tubes smoothes potential stiff points. The friction coefficient between the ring and the mounting is investigated as well. Eventually, several observations are made which lead to design recommendations for fatigue sizing of the slewing bearing screwed joints.

Keywords Bolted joint · Slewing bearing · Preloading · Fatigue · Finite element method

Z. Chaib (✉) · A. Daidié · D. Leray
Laboratoire de Genie Mecanique de Toulouse (LGMT),
135 Avenue de Rangueil, 31077 Toulouse, France
e-mail: zouhair.chaib@insa-toulouse.fr

A. Daidié
e-mail: alain.daidie@insa-toulouse.fr

D. Leray
e-mail: dimitri.leray@insa-toulouse.fr

1 Introduction

Slewing bearings provide compact designs for pivot linking and driving. Assembling to the structures is achieved using bolts or screws. Most of the time, slewing bearings are used for low-speed motions (e.g., cranes, trackers, wind-turbines). However, they have to carry very high and variable cyclic efforts [1]. The loading may be broken down into thrust load, radial load and moment which is often significant for sizing the bearing [2–5].

In order to ensure integrity of the whole structure, fatigue has to be mastered for each component of the assembly (screws, rollers, rings, ...). Zupan [6] and Amasorrain [7] studied the strength of the rolling elements in order to determine bearing load capacity. They proposed procedures that can be used to evaluate the load distribution for the rollers. In the cases when the surrounding structures are very stiff, it can be admitted that the distribution follows a sine pattern. In the other cases, the rings distort and the distribution shows peaks, for example near stiffeners. Sine-patterned distribution may then be questioned [6,8].

Several works [1,9,10] have shown the difficulty in sizing the bearings' joints and dealt with the behavior of the screws. Those are mainly loaded with bending and behave a very non-linear way [11]. The behaviour is related to geometrical characteristics of the surrounding structures. Limitations of the analytical models used to describe the behavior of this kind of assembly were also investigated (VDI design guidelines [12]; Bent beam model [13,14]). The first one is the most usual model among slewing bearing manufacturers. It assumes that the assembled parts do not separate under loading, i.e., each ring on its mounting. Experiments show that this is not true [9,10,15]. The second model deals with slender

structures, which is not the case we are concerned with. This leads us to develop several numerical simplified models [16–18]. Those only deal with bolted joints (i.e., using screws and nuts); the content is not detailed here.

At some industrial companies' request, which specialise in handling and lifting equipment, and collaborating with CETIM, we extend our works to screwed joints (i.e., tapped parts) of slewing bearings. The developments lead us to elaborate parameterized 3D finite element models. The results of those are compared to experimental results. Experiments and numerical simulations are presented hereafter. Then the effect of some geometrical and technical parameters is investigated, aiming at better sizing the screwed joints of slewing bearings.

2 Experimental study

2.1 Test mounting

The setup shown in Fig. 1a reproduces an industrial environment for the bearing. The most typical configurations of bearing assembly were chosen. A hydraulic actuator loads the end of the arm. The loading breaks down into moment M_T and thrust load F_A. The bearing used features 72 screws uniformly distributed on the rings. Each ring has 36 screws (M16, grade HR 10.9), 6 of which are equipped with uniaxial strain gauges. The equipped screws were located according to Fig. 1b. That allows evaluating the load distribution in the joint. Symmetry of the joint loading may also be checked.

2.2 Studied assemblies

Several configurations were tested. The choice of configurations resulted from a survey among manufacturers and users of slewing bearings. Figure 2 sums up the most typical configurations. The first assembly features tapped mountings. The second one uses tapped rings. Here the screws tighten the mounting plate against the ring. One drawback of that assembly lies in the fact that the screws are short, thus the cyclic loading is higher. The most often used and most economical remedy lies in adding spacers (Fig. 2b). Screw rigidity is reduced. This lessens possible stiff points and makes load distribution more uniform.

3 FEM analyses

From here, we only deal with the two assemblies of Fig. 2. Presented hereafter are the numerical models which

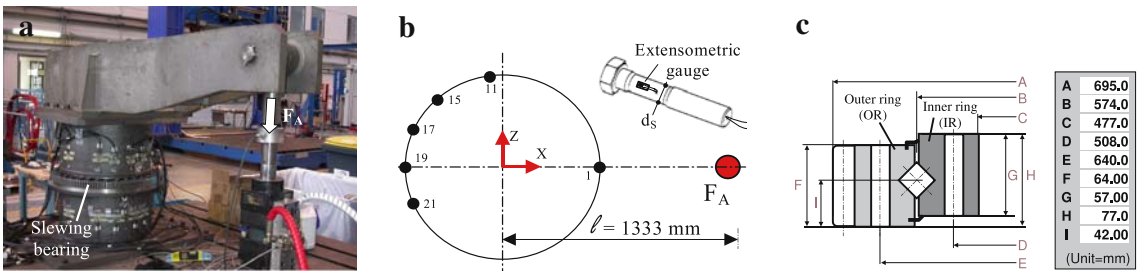

Fig. 1 Test bench: **a** test bench, **b** location of the instrumented screws, **c** slewing bearing characteristics

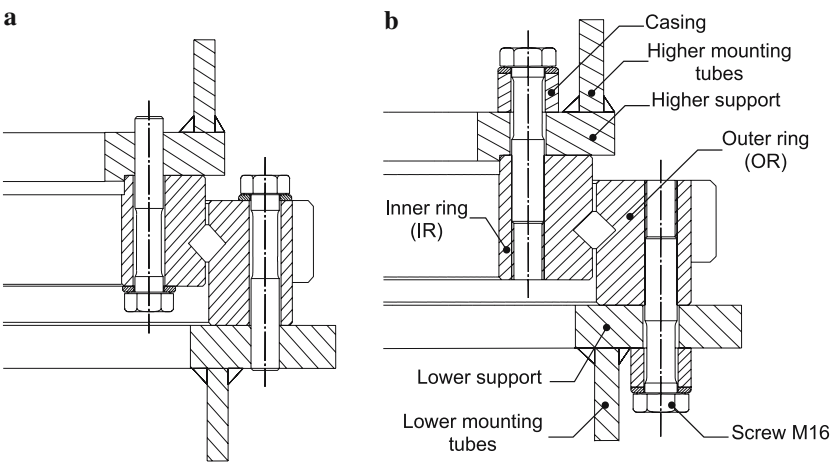

Fig. 2 Studied assemblies: **a** ring screwed to support, **b** support screwed to ring using cylindrical casing

were used to better understand the behavior of the joints. The first step consists in validating the finite element models using experimental results. Secondly, geometrical and physical parameters are changed in order to analyse the assembly's behavior sensitivity to them.

3.1 Three-dimensional FE model

Geometrical symmetry of the assembly allows reducing the modeled volume to the most loaded angular sector, although the loading does not comply to the symmetry. Actually, Schaumann [19] and Chaib [20] pointed that reducing to this angular sector and using an equivalent loading gives safe results which are very close to those obtained with models of the whole structure. Moreover, processing and computing times are obviously much lower. The benefit is high too if the influence of geometrical or physical parameters has to be investigated. Eventually, reducing the model with this technique affords the possibility to build local models which reveal much more efficient than models of half the structure.

Leray [10] showed that the behavior of the joint of one ring is independent of the configuration of the other ring, via an experimental study. Sizing a slewing bearing assembly then reduces to one study for the outer ring (model of an angular sector of the outer ring and its mounting), and a second study for the inner ring (see Fig. 3a–c). In that case, the key data to be evaluated is the load distribution Fe carried by the rollers.

3.2 Fe loading

The load distribution Fe is highly dependent upon the stiffnesses of the mountings. The test bench includes

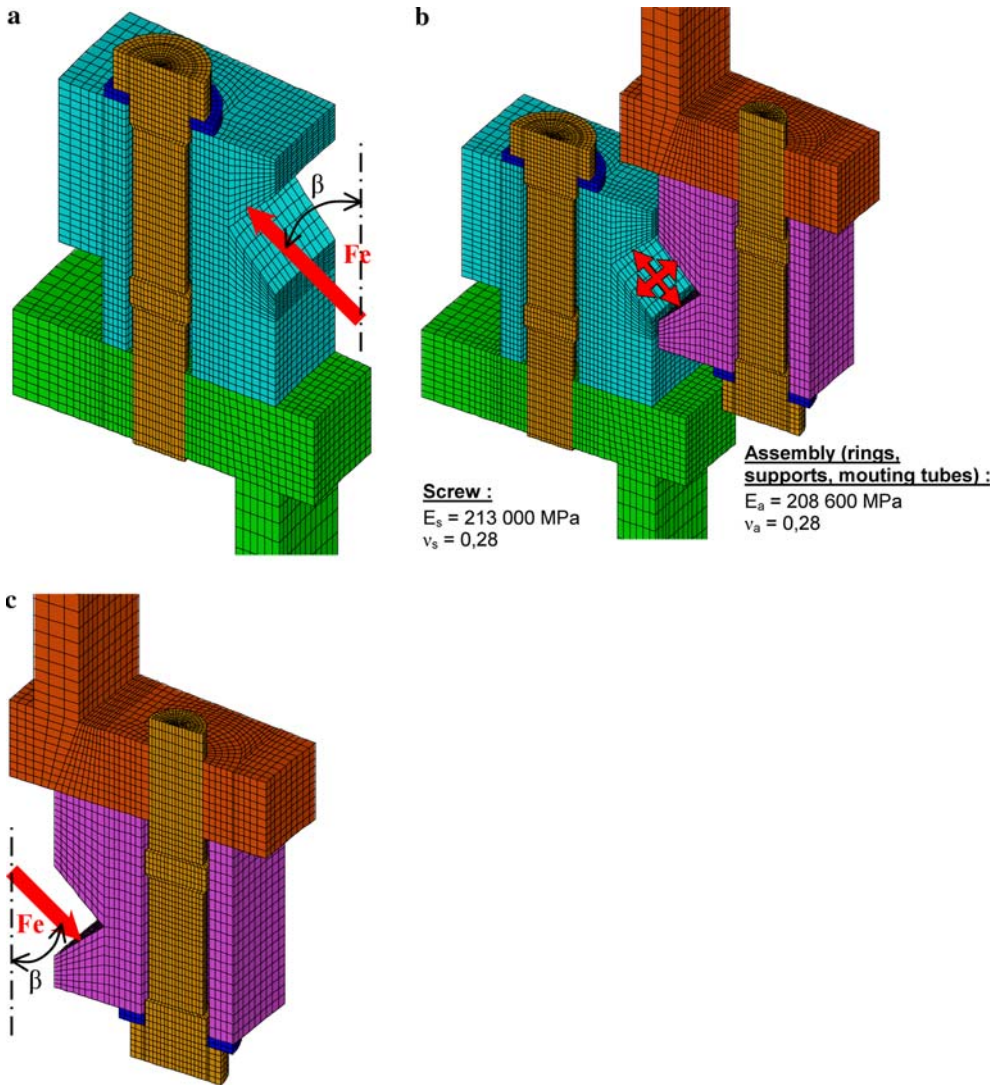

Fig. 3 FEM mode: **a** outer ring, **b** 3D FEM model of slewing bearing, **c** inner ring

cylindrical mounting tubes. This shape offers the advantage of filtering the induced load in the structure. This will be discussed further in Sect. 4. This design eventually makes the load distribution on the roller tracks closer to a sine distribution.

3.2.1 Equivalent load calculation

In the case when the loading follows a sine distribution, the equivalent load (Fe) applied on the most loaded angular sectors (sectors of screw ♯1 and ♯19) is defined by Eq. 1. According to Vadean [9], this is used by most sizing procedures for bolted joints of slewing bearings. The sine distribution is often assumed in offshore construction, when tubes are loaded by a bending moment [21].

$$Fe = \frac{1}{\cos\beta}\left(\frac{F_A}{Z} + \varepsilon\frac{2M_T}{\pi R}\sin\frac{\pi}{Z}\right) \tag{1}$$

with Z number of screws,
R radius of roller load location (application point of F_e),
β angle between F_e and the axis of the bearing,
$\varepsilon = 1$ for screw ♯1, and $\varepsilon = -1$ for screw ♯19.

3.2.2 Loading range

The actuator is operated up to 120 kN, which is slightly less than the strength of the slewing bearing. The moment is computed using the distance between the axis of the bearing and the axis of the actuator: $M_T = l.F_A$. The test setup allows tension and compression loading. Figure 4 recaps all simulated cases, that correspond to test bench configurations. The slewing bearing used is a crossed roller bearing. Every other roller is loaded at a time; contacts between tracks and rollers change depending on the loading.

3.3 Behavior of the screw

Fatigue strength of a screw hardly depends on average loading level. Limit alternate stress ($\sigma_{a_{adm}}$) is admittedly the same whatever the preload intensity. The limit alternate stress is taken as 50 MPa for the screws of the test setup [22]. The alternate stress in a screw can be computed from the load variation (ΔFb) and the moment variation (ΔMb), i.e., the difference between preload and maximum load. Equation 2 sums up the

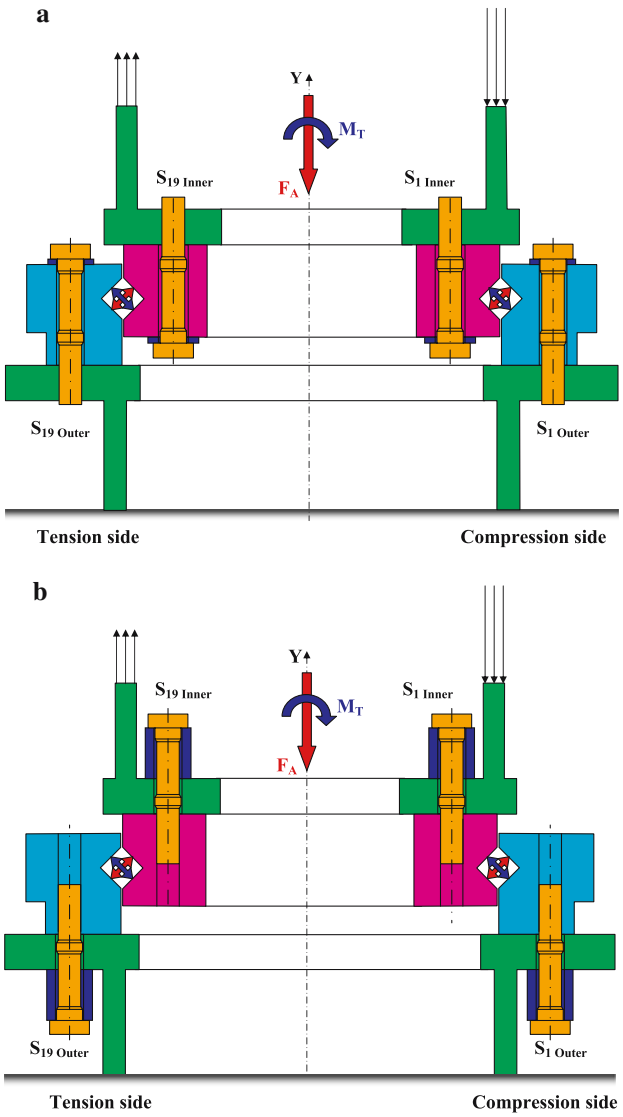

Fig. 4 3D FE models

calculation.

$$\sigma_a = \frac{\Delta\sigma_{YY}}{2} = \frac{\Delta Fb}{2A_s} + \frac{\Delta Mb.d_s}{4.I_s} \tag{2}$$

with A_S, d_S and I_S, respectively area, diameter and quadratic moment of the bolt's section.

Tension load Fb (or variation ΔFb) is uniform along the screw, whereas bending moment (or variation ΔMb) varies linearly (see Fig. 5). Fatigue sizing requires to determine the weakest section of the screw. In a uniform-section region, the most loaded section is the nearest from the engaged threads. Experiments lead us to fix the strain gauges 15 mm under the screw's head. That location is not the most interesting one, nevertheless the stresses can be extrapolated to any other section.

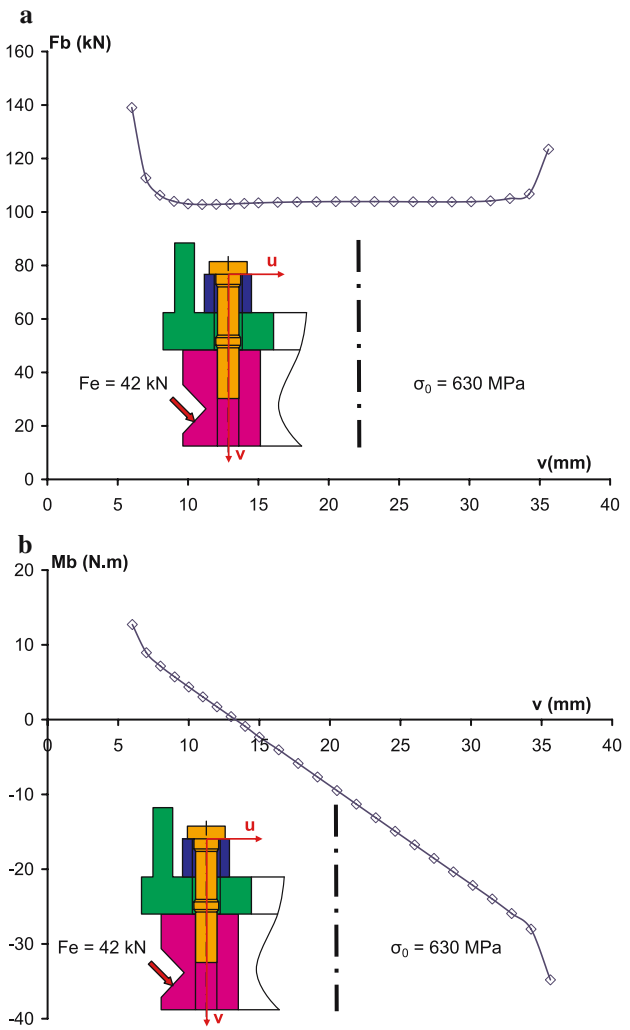

Fig. 5 Tension load and bending moment in the screw (F_A = 120 kN)

Moreover, the comparison between experimental measures and simulation results will be achieved at the location of the gauges.

3.4 Validation of the numerical simulations

Figures 6 and 7 compare numerical simulation results and experimental results.

The hypothesis of sine-distributed rolling track efforts implies that the screws located in the symmetry plane should be the most loaded, i.e., screws ♯19. The numerical simulations are based on the data of screw ♯19.

Several points have to be noted here.

Under tensile loading, the stress of the screws is highly non-linear (screw ♯17), whereas under compressive loading, the stress is linear (screw ♯1). The latter is related to the fact that the efforts are carried right from the ring to the mounting. In that case, the alternate loading of the screws is the lower. In the case of tensile loading, the screw carries the whole loading and it is subjected to bending (Fig. 8). Furthermore, a gap may appear between the ring and the mounting plate. Screw ♯21 is more loaded than reference screw ♯19. Moreover, the measures for screws ♯17 and ♯21 are quite different, which reveals that the setup is not exactly symmetrical. However, it must be reminded that the accuracy of bolt preloading and the tightening procedure might cause important measurement uncertainty. Moreover, the fact that the whole structure slightly shrinks under loading may be another cause. It appears that the joint of either ring behaves very differently. The screws of the inner ring are much more loaded than those of the outer ring. This is due to the location circle's radius which is lower for the inner ring, although the same moment Mt is carried. Additionally, the alternate stress is higher for tension loading than compression loading. As noted above, this is related to the fact that the load is carried directly by the mounting in the case of compression. 3D finite element (FE) results correlate well to experimental results for tension loading. Under compression, 3D FE models reproduce the shape of the stress curves (linear behaviour) and give higher stresses than experiments. The difference is mostly due to the model of the external load which is higher than the real loading.

4 Discussion about the main parameters

The simulation method was checked against experimental results and validated. Now the influence of several parameters is studied:

- preload intensity,
- height of the bushes,
- position of the mounting tubes,
- friction coefficient.

This is done via numerical simulations of the angular sector of screw ♯19, using a parameterized model. Only the inner ring is studied, as it is the most loaded ring according to Figs. 6 and 7.

4.1 Influence of the preload intensity

Several authors showed analytically, numerically and experimentally [10,13,14] the advantages of a high preload ($\sigma_0 \approx$ 70–80% of Re). However, the assembling procedure and the tightening equipment have to be taken into account, as the real value of preload can not be known with high accuracy. Using an electronic torque

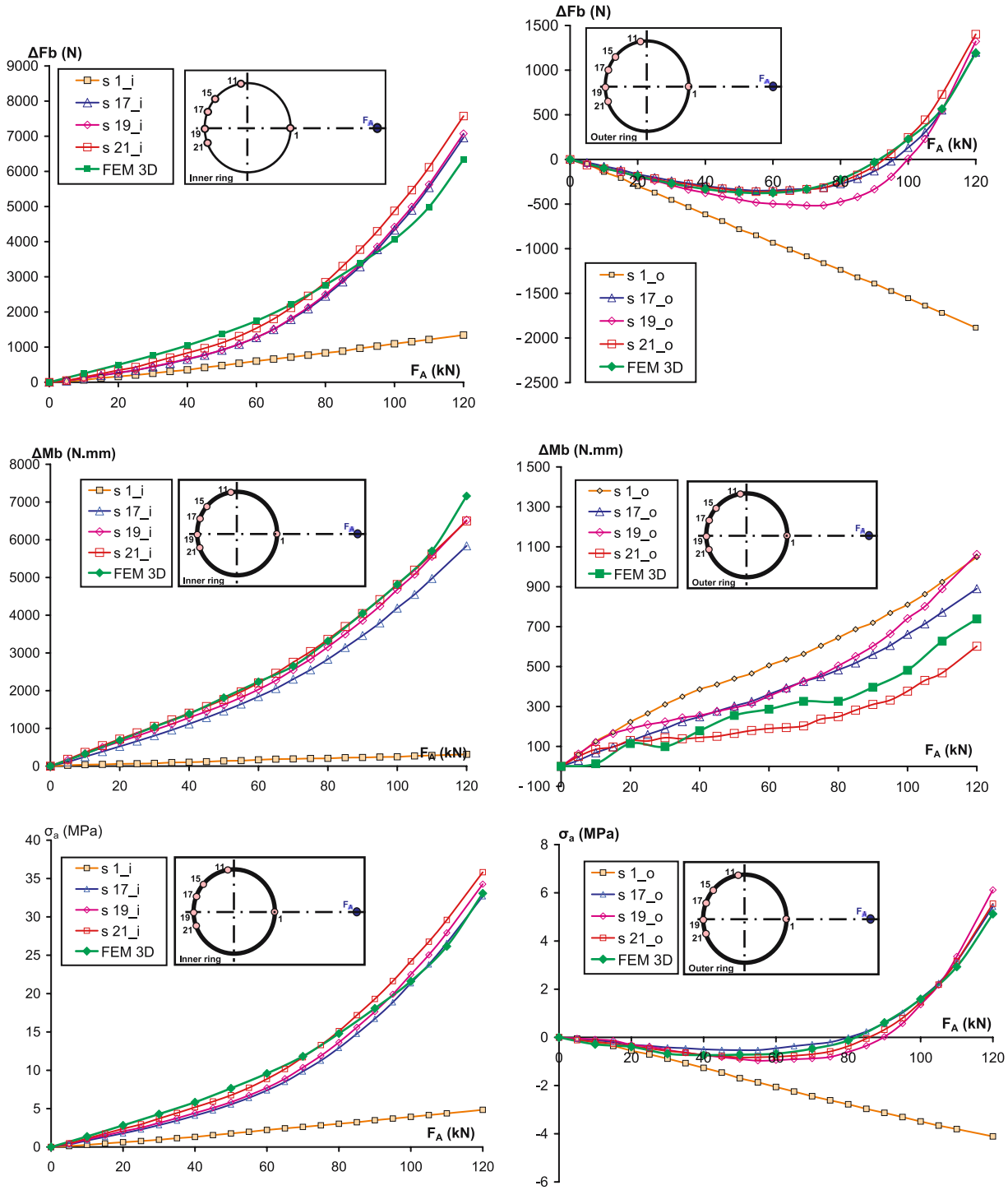

Fig. 6 Three-dimensional FE results and experimental results (assembly ♯1)

wrench, the accuracy on torque is ±5%. Only 10% of the torque really participates in installing the tensile load. The rest of it is used to overcome friction. Eventually, with that equipment, the accuracy on the preload σ_0 is ±20%. That makes an uncertainty coefficient $\alpha_i \approx 1.5$ [12,22].

Figure 8 shows the benefit of preloading as much as possible, without reaching yield stress under maximum loading. Indeed, a high preload enables to:

1. reduce alternate stresses (Fig. 8a),
2. reduce the risk of loosening [12],
3. lag the beginning of slipping (Fig. 8b).

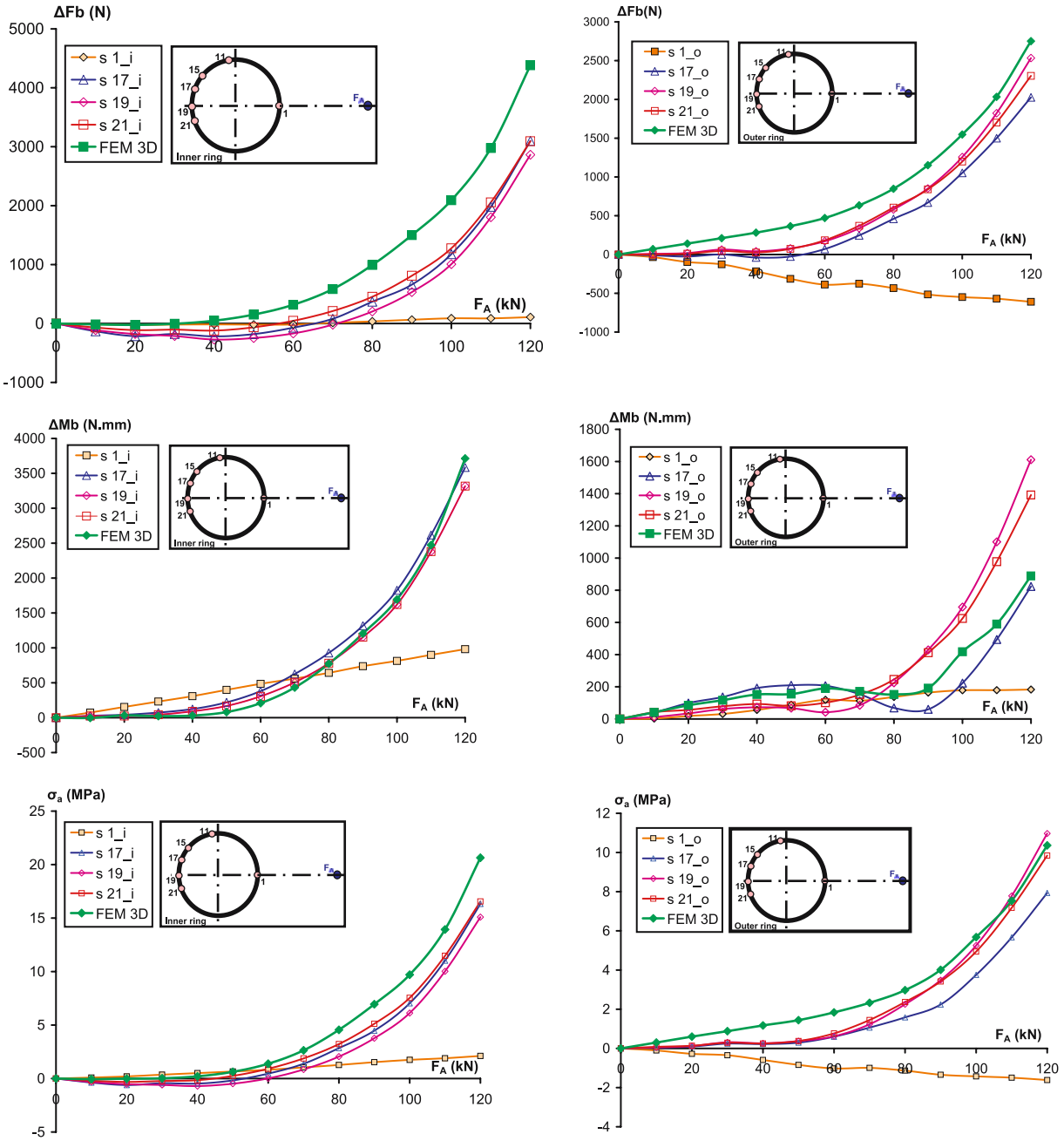

Fig. 7 3D FE results and experimental results (assembly ♯2)

With the tightening equipment used here, the range of preload intensity varies of 50–70%. Figure 8a indicates that there is no significant difference up to the local load of $Fe = 25$ kN. Beyond that, the uncertainty on the tightening intensity has a major influence on the alternate stresses.

4.2 Influence of the bushes' height

The strength of the bolted assembly highly depends on the stiffness of the screw and the stiffness of the assembled parts. Moreover, factor γ, which characterizes the location of the external load along the axis of the screw ($\gamma = h/H_P$) has a direct influence on static and fatigue strength of the joint [12,14] (Fig. 9). The lower γ, the higher the strength of the assembly. Using bushes is a way to use longer screws, thus to reduce their stiffness. Then it improves their fatigue strength [20]. It also reduces the risk of self-loosening. Taking this problem into account leads all slewing bearing manufacturers, as well as VDI design guidelines [12], to advise that the height (H_P) over diameter ratio be more than 3 to 5.

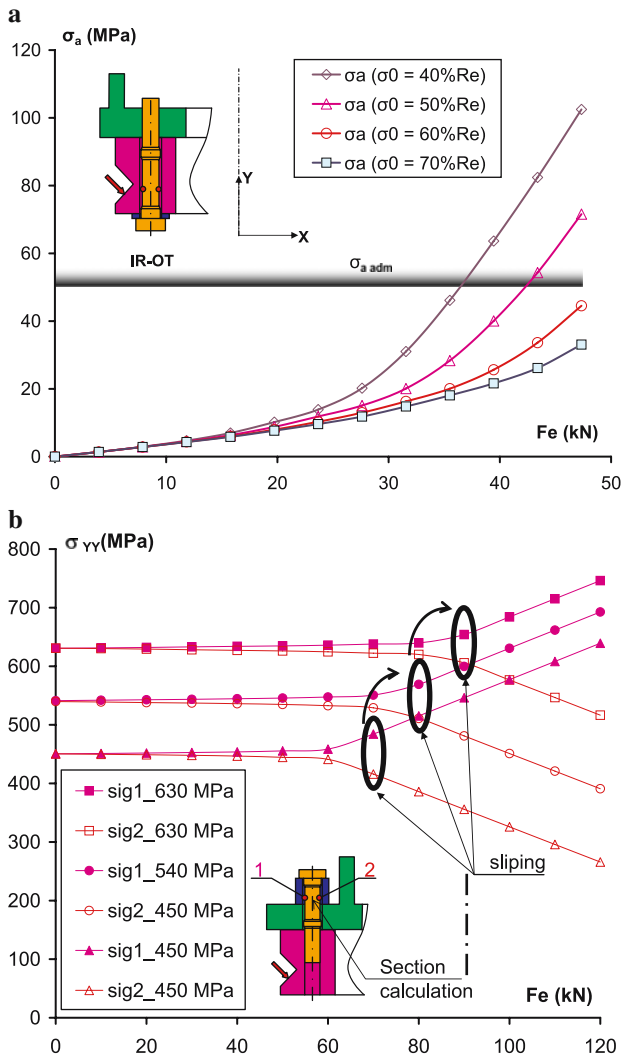

Fig. 8 Influence of the preload intensity

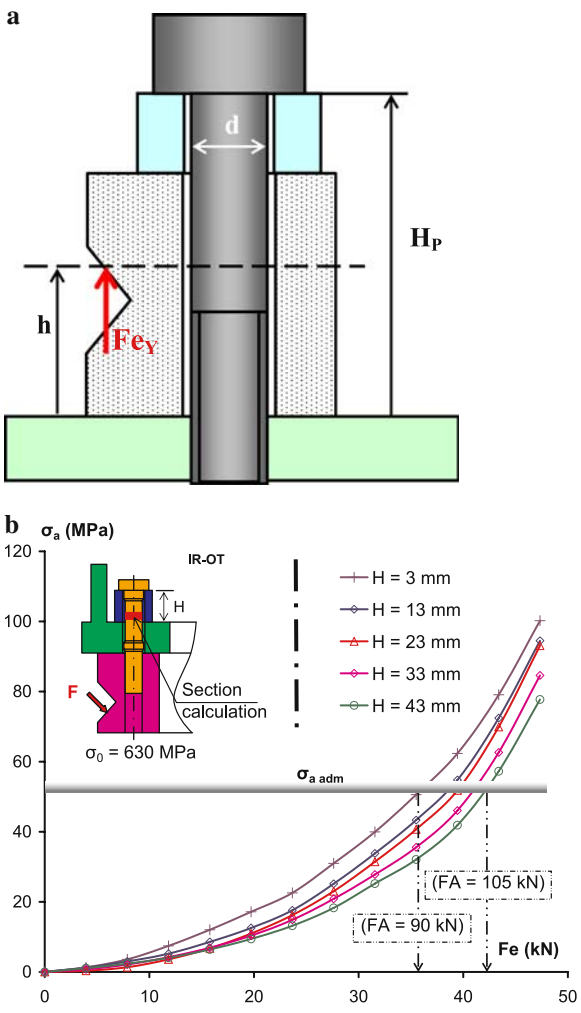

Fig. 9 Influence of the height of bushes on the alternate stress

In order to evaluate the influence of the bushes' height, five values were used for it (3, 13, 23, 33 and 43 mm). The values of computed stress correspond to the first engaged thread. Those were extrapolated from values computed in elements located far away from any change in section, in order to avoid stress concentration effects. It must be noted that all computed stresses do not take into account the presence of the threads. The threaded part of the screw is modeled with a smooth cylinder. Figure 9 shows the benefit that can be brought by using long bushes. The study shows that using 43 mm instead of 3 mm allows to raise the maximum loading from 90 to 105 kN.

4.3 Influence of the mounting tube's geometry

Using mounting tubes reduces stiff points caused by a complex structure. Amasorrain [7] showed that some load peaks are due to the elasticity of the rings. However, the way each ring is fixed can cause peaks too. The phenomenon may bring oddly-distributed bending directions for the screws (Fig. 10).

4.3.1 Influence of the tube's height

Changing the height of the tube has no direct influence on the loading of the screws. Raising the height smoothes the load distribution on the bearing, and progressively erases stiff points (Fig. 11).

Feet were added under the tube, as shown by Fig. 11, in order to emphasize stiff points. The graphs show that the tube acts as a filter that smoothes the loads carried by the feet.

The first case of Fig. 11, with perfect clamping of the tube, validates the hypothesis of sine-distributed load in the bearing.

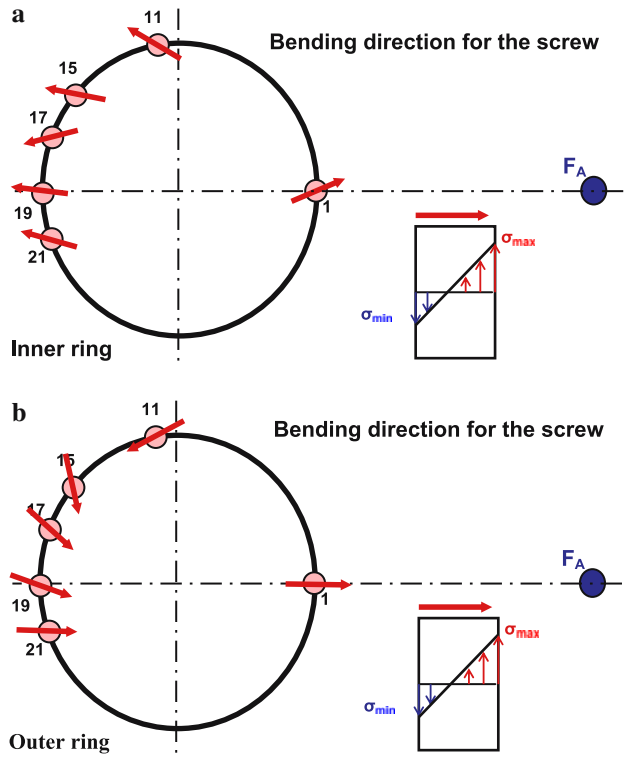

Fig. 10 Bending direction for each screw ($F_A = 120\,\text{kN}$)

4.3.2 Influence of the tubes position

The position of the mounting tubes has a direct influence on the behaviour of the screws. The position that minimizes bending is the one for which the tube's diameter equals the average diameter of the bearing. For inner rings and outer rings, if the screws are located between the rollers and the mounting tubes, there is a high risk of slipping between the ring and the mounting (Fig. 12).

Slipping can be reduced different ways:

- by raising the preload, if the screws are strong enough;
- by using more screws, if the design and the assembling procedure allow for it;
- by changing adherence parameters such as surface rugosity.

Or it can be avoided using centering or pins.

If no solution of the kind is chosen, the assembly will not be reliable considering slipping. Moreover, it may be uncomfortable to the users as slipping may produce slaps.

4.4 Influence of the friction coefficient

Figure 11 shows that the higher the friction coefficient, the more stable the assembly and the less the risk of slipping between ring and mounting. Practically, friction coefficients may be modified either via a change in the roughness of contact surfaces (Fig. 13), or by using glue.

5 Conclusion

This study first allowed us to compare the behaviour of the screws for experiments and for numerical simulations.

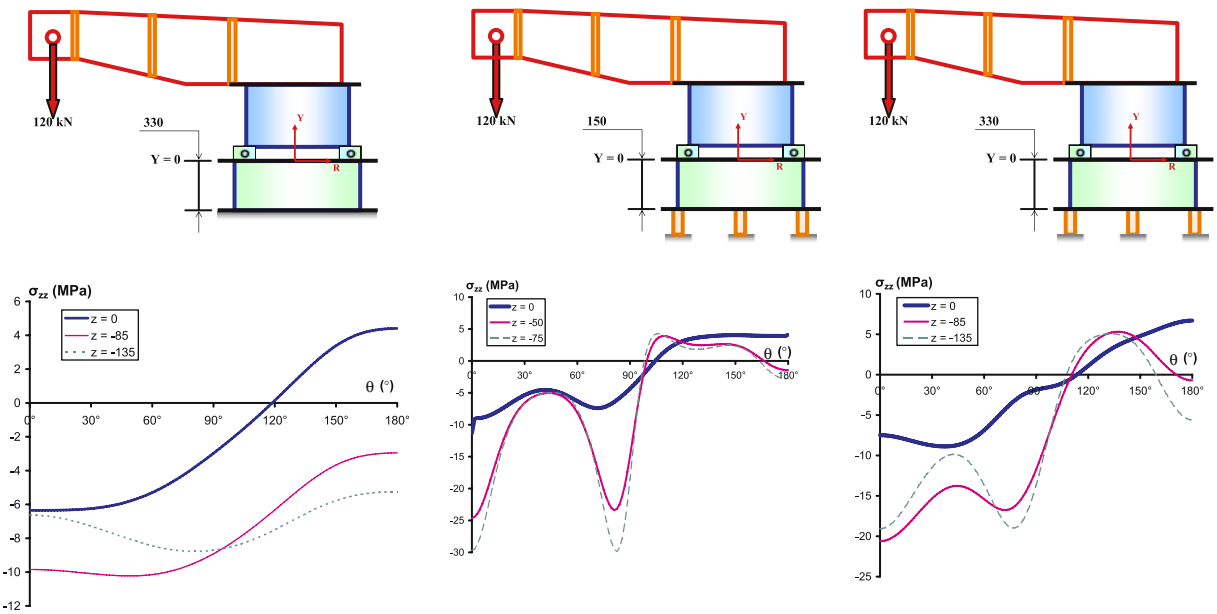

Fig. 11 Influence of the tube's height

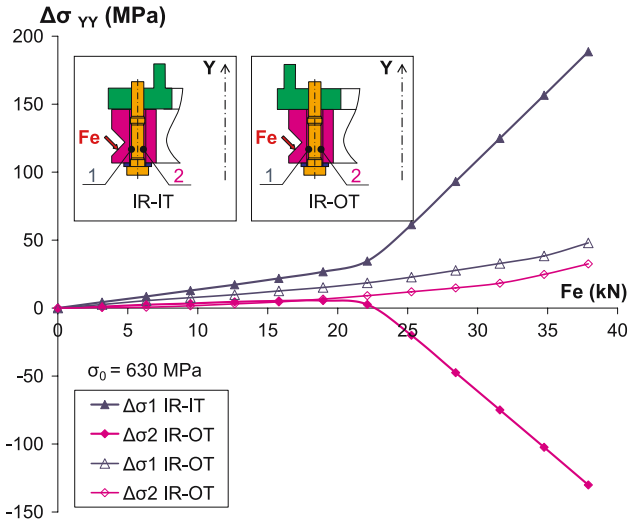

Fig. 12 Influence of the tubes' position

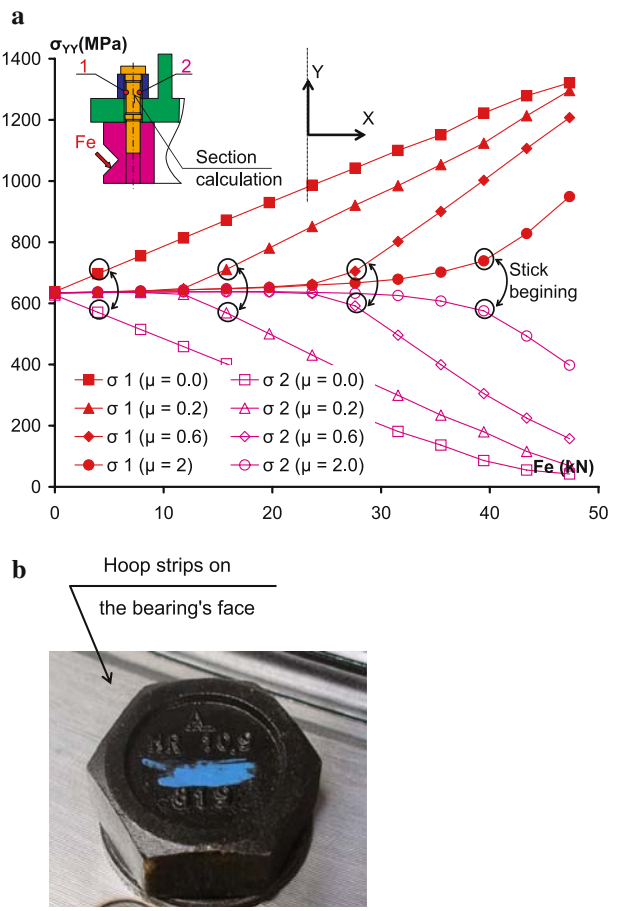

Fig. 13 Influence of the friction coefficient

The numerical models were parameterized in order to evaluate the influence of some geometrical and physical data on the loading of the screws. A panel of solutions is proposed to enhance the fatigue strength of the joints. Optimising such assemblies is indeed a very complex and expensive task using 3D FE.

However, studying assemblies for which the sine-distributed loads hypothesis is not applicable will require this type of modeling. This will be possible via a multi-scale method: first a study of the whole structure, then a local and detailed analysis related to the environment of the bearing. Switching from the first model to the second then has to comply with compatibility conditions. These works are one of the main focuses of our future research.

References

1. Dalhoff, P., Frese, T.: Fatigue analyses of bolted and welded joints, practical experience in type certification of wind turbines. NAFEMS seminar fatigue analysis, Wiesbaden, 8–9 November, pp. 1–18 (2000)
2. Kaydon: Large bearing design manual and product selection guide, vol. catalog 390. http://www.turntablebearings.com
3. PSL: Slewing rings, production programme. CD Publ.9/2001-OTO-A, ISBN 80-88889-38-3. http://www.psl.sk
4. Rollix-Defontaine, S.: slewing rings and special bearings, vol. catalog indice 4. March 2002 (2002). http://www.rollix-defontaine.com
5. Rothe Erde.: Rothe Erde slewing bearings, vol. 1332. http://www.rotheerde.com
6. Prebil, I., Zupan, S.: Carrying angle and carrying capacity of a large single row ball bearing as a function of geometry parameters of rolling contact and supporting structure stiffness. Mech. Mach. Theor. **36**, 1087–1103 (2001)
7. Damian, J., Amasorrain, J.I., Sagartzazu, X.: Load distribution in four contact-point slewing bearing. Mech. Mach. Theor. **38**, 479–496 (2003)
8. Reymond, J.C.: Utilisation de la boulonnerie hr dans le cadre des grues à tour, pp. 281–295. Saint-Etienne, France, CETIM Saint-Étienne, 25–26 October 1995
9. Vadean, A.: Modélisation et simulation du comportement des liaisons par éléments filetés de roulements de très grand diamètre. Ph.D. thesis, INSA de Toulouse, Toulouse, France (2000)
10. Leray, D.: Outil de dimensionnement de fixation boulonnée de couronnes d'orientation. Ph.D. thesis, INSA de Toulouse, Toulouse, France (2002)
11. Massol, J.: Fixations des couronnes d'orientation. revue CETIM-Informations, n172, pp. 47–49, Février (2001)
12. VDI 2230 BLATT 1. Systematische berechnung hochbeanspruchter Schraubenverbindungen Zylindrische Einschraubenverbindungen, chapter VDI Richtlinien, VDI-Gesellschaft Entwicklung Konstruktion Vertrieb, Fachberuch Konstruktion, pp. 1–169. ICS 21.060.10. Ausschuss Schraubenverbindungen, Febuary 2003
13. Agatonovic, P.: Beam model of beam flanged connections. Eng Comp, vol. 2, pp. 21–29. Pineridge press ltd edition, Swansea (1985)
14. Guillot, J.: Assemblage par éléments filetés; modélisation et calculs, vol. Tome 1 B5560 à B5562, 75006, pp. 1–56. France, Paris, Techniques de l'ingénieur edn (1987)
15. Massol, J.: Calcul de fixations de couronnes. Technical report 120281-120282-120283, CETIM Saint-Étienne, Saint-Étienne, France, May 2000

16. Guillot, J., Vadean, A., Leray, D.: Bolted joints for very large diameter bearings—numerical model development. Finite elements in analysis and design, pp. 1–13. August 2005
17. Combes, B., Leray, D., Daidié, A.: Rapid simulation of preloaded bolted assemblies for slewing bearings. In: ASME IMECE2001, pp. 1–11. ASME IMECE2001, ASME publication number H1229D, New York, 11–16 November 2001
18. Guillot, J., Mathieu, A., Daidie, A., Leray, D.: Mise en oeuvre d'un logiciel de calcul dédié aux fixations boulonnées de couronnes d'orientation de grue de levage. In: Journée technique, pp. 1–10. CETIM Saint-Étienne, Saint-Étienne, France, 21 September 2004
19. Kleineidam, P., Schaumann, P.: Global structural behaviour of ring flange joints. In: NAFEMS seminar: modelling of assemblies and joints for FE analyses, pp. 1–9. Wiesbaden, 24–25 April 2002
20. Guillot, J., Chaib, Z., Daidié, A.: Calcul d'une fixation boulonnée en fatigue, pp. 1–12. CMSM'2005 (first international congress design and modelling of mechanical systems) Hammamet, Tunisie, 23–25 March 2005
21. Brink, H.J., Deekker, C.J.: External flange loads and 'koves'-method, pp. 145–155 (2002)
22. NORME E25–030. Fasterners. Threaded connections. Design, calculation and mounting conditions, pp. 1–73. AFNOR Publications, Paris, August 1984